23rd International Conference on
Harmonisation within Atmospheric Dispersion Modelling for Regulatory Purposes
15-19 September 2025, Hamburg, Germany

EXTENDED ABSTRACT

Improvements in local-scale turbulence modelling in the PMSS flow model with applications to natural and built environments

Bruno RIBSTEIN – SUEZ ARIA Technologies, F-92000 Nanterre, France - bruno.ribstein@suez.com
Patrick ARMAND & Christophe DUCHENNE – CEA, DAM, DIF, F-91297 Arpajon, France
Maxime NIBART & Armand ALBERGEL – SUEZ ARIA Technologies

Abstract: Atmospheric releases, such as radionuclides or chemicals, can disperse over distances from a few to thousands of kilometers. However, most impacts are usally confined to the near field, within a few kilometers, making accurate simulation of flow and dispersion in this zone critical. Near-field turbulence is influenced by local obstacles (e.g., buildings, topography) and larger-scale meteorological conditions. To address these complexities, the PMSS system, combining the 3D diagnostic flow model PSWIFT and the 3D Lagrangian particle dispersion model PSPRAY, operates at metric resolution and explicitly accounts for obstacles. Local turbulence is modeled as a combination of background atmospheric and obstacle-induced components. Implementation is reviewed and validation was conducted in two synthetic environments: a forest in open fields and a cubic obstacle, analyzing 3D wind fields and turbulence profiles. Results confirm the robustness of the models, which can be applied beyond PMSS, balancing accuracy and computational efficiency.
Key words: *PMSS modelling system, canopy parametrisation, experimental validation, Cube (CEDVAL).*

INTRODUCTION

Precise evaluation of the spatial and temporal distribution of gases and/or airborne particles requires an accurate description of the transport and dispersion of these species. In crisis situations, a compromise is necessary between accuracy and computational time.

The PMSS (Parallel-Micro-SWIFT-SPRAY) system combines the 3D diagnostic flow model PSWIFT and the 3D Lagrangian particle dispersion model PSPRAY. It aims to provide results close to the accuracy of CFD models with significantly faster computation times (Tinarelli et al., 2013; Armand et al., 2021; Oldrini et al., 2019; 2021).

Turbulence allows the transfer of energy between large-scale eddies and smaller ones. The Atmospheric Boundary Layer (ABL) describes the thickness of the atmosphere influenced by soil-atmosphere (or ocean-atmosphere) exchanges, in particular exchanges of heat, momentum, and moisture, and whose surface boundary layer (SBL) is the sublayer near the ground with strong vertical gradients of average quantities (velocity, temperature, and humidity).

This article follows Ribstein et al. (2024), describing the implementation in PSWIFT of Monin and Obukhov's (1954) similarity theory in the SBL. The present paper revisits the modeling in PSWIFT of turbulence characteristics in the ABL. Three commonly used parameterizations are presented, avoiding the presentation of a fourth consisting of interpolating the turbulence prescribed by a larger-scale model. The parameterizations are evaluated, first on the cube case, modeled in the wind tunnel at the University of Hamburg, then on an academic case of a forest in the middle of grassland. The latter case is used to review the parameterization of the wind attenuation in a vegetation canopy.

LARGE-SCALE TURBULENCE PARAMETERIZATION

Hanna et al. (1982) suggest empirical relationships to provide typical wind fluctuations in the ABL, with a dependence on the dynamic stability of the atmosphere. These relationships are implemented in PSWIFT, assuming horizontal isotropy of fluctuations, to parameterize the Lagrangian timescales (τ_h ; τ_z) and standard deviation of velocities (σ_h ; σ_z). The parameters are the turbulent friction velocity u_*, the buoyancy velocity w_*, the boundary layer thickness h_{mix}, the Monin-Obukhov length L_{mo}, and a parameter $f = 10^{-4} \cdot \mathrm{s}^{-1}$.
Until version 2.3.0 of PSWIFT, only L_{mo} controlled atmospheric stability. In version 2.3.1, and in accordance with Golder's formulation (1972), atmospheric stability also depends on roughness, with version 2.3.0 corresponding to the limiting case of roughness greater than 0.5m. As indicated in Table 1 for the Prairie Grass experiments, this update corrects an inconsistency between the stability deduced from the L_{mo} estimated by Horst et al (1979) and that chosen by PSWIFT.

Table 1: Four cases from the Prairie Grass experiment, Pasquill class based on L_{mo} estimated by Horst et al (1979) and by PSWIFT

Experiment	L_{mo} in m	Pasquill class	PSWIFT 2.3.0	PSWIFT 2.3.1
14	7.6	F	Stable	Stable
17	50	E	Stable	Stable
24	217	D	Stable	Neutre
57	-189	D	Instable	Neutre

SMALL-SCALE TURBULENCE PARAMETERIZATION

The size of the eddies, defined by the mixing length l_m, determines the efficiency of dispersion of materials. In PSWIFT, the length l_m is modeled semi-empirically, assuming a steady-state mixing layer where turbulence production balances dissipation. Near the ground, the distance to the nearest obstacle limits l_m, with a linear relationship up to a maximum distance of 100m. The proportionality parameter ($C_1 = 0.08$) allows l_m to be approximately equal to one tenth of the thickness where velocity variations are significant. Energy dissipation ϵ is assumed to be equal to energy production, i.e., $\epsilon = 2 \cdot \upsilon_t \cdot \|\tau\|^2$, noting υ_t as the turbulent viscosity and $\|\tau\|$ the norm of the strain tensor. A turbulent closure equation defines $\upsilon_t = l_m^2 \cdot \|\tau\|$ (Smagorinsky, 1963). Assuming isotropic turbulence, Rodean (86) links υ_t and ϵ to standard deviation of velocities ($\sigma_{lm}^2 = \sqrt{C_0} \cdot l_m^2 \cdot \|\tau\|^2$) and Lagrangian timescales ($\tau_{lm} \cdot \sqrt{C_0} \cdot \|\tau\| = 1$).

One limitation of the mixing length parameterization is the absence of turbulence in the absence of a gradient ($\|\tau\| = 0$). In addition, the analytical description of the influence of buildings on the flow leads to significant gradients in the diagnostic version of PSWIFT. PSWIFT therefore constrains the variations of τ_{lm} to the interval [1;100] seconds.

The norm $\|\tau\|$ is defined as the sum of the strain elements $2 \cdot \epsilon_{ij} = \partial_i u_j + \partial_j u_i$, noting (1=x, 2=y, 3=z): $\|\tau\|^2 = \epsilon_{11}^2 + \epsilon_{22}^2 + \epsilon_{33}^2 + 2 \cdot (\epsilon_{21}^2 + \epsilon_{31}^2 + \epsilon_{32}^2)$. The strain elements ϵ_{ij} are defined by finite differences and an average over the four points of the neighboring meshes. A typo in version 2.3.0 causes the vertical gradients to contribute four times too much. This is corrected in version 2.3.1.

TURBULENCE PARAMETERIZATION

Hanna et al. (1982) provide typical values for large-scale turbulence (σ_{Hanna}, τ_{Hanna}), while the mixing length formulation provides small-scale induced turbulence (σ_{lm}, τ_{lm}). This third parameterization (σ_{som}, τ_{som}) underlying assumption is the decorrelation of the two previous types of turbulence. In the ABL, the parameterization sums the standard deviations ($\sigma_{som}^2 = \sigma_{Hanna}^2 + \sigma_{lm}^2$) and turbulent diffusivities to estimate the Lagrangian timescales ($\tau_{som} \cdot \sigma_{som}^2 = \sigma_{Hanna}^2 \cdot \tau_{Hanna} + \sigma_{lm}^2 \cdot \tau_{lm}$).

The parameterization is used in the following validation cases.

HAMBURG WIND TUNNEL CUBE

The 3D turbulence parameterization is compared with observations from the wind tunnel at the University of Hamburg for an obstacle elongated along the flow ($L \times W = 0.8 \cdot H \times 1.2 \cdot H$), with a height $H = 25m$. The numerical modeling in a neutral atmosphere ($|L_{mo}| > 2500m$) covers an area of 378m×200m at a horizontal resolution of 2m, and a uniform vertical resolution of 2m up to $4 \cdot \mathrm{H} = 100\mathrm{m}$.

Figure 1 shows the profiles of the vertical wind and the component along the flow. For the profile extracted at X=1.56·H, the velocity U shows a change of sign from $z \geq 0.5 \cdot H$, which PSWIFT could model by slightly shortening the length of the cavity (Fackrell, 1984). Note the absence of acceleration of the modeled U component above the building ($H \leq z \leq 2 \cdot H$) and the absence of modeled $W > 0$ in the layer $z \leq H$. At both extraction locations, the modeled U shows a slight underestimation (slope of 0.91 for a correlation coefficient R>0.95 if the trend is forced to intersect the origin). The modeled W shows a more significant underestimation (slope of 0.61 or 0.67 for a correlation coefficient R>0.93).

The roughness $z_0 = 0.1 \cdot H = 0.25m$ is chosen so that large-scale turbulence parameterization represents correctly the observations. Figure 1 shows the horizontal standard deviation σ_h for the two versions of PSWIFT. The figure illustrates the importance of vertical gradients in the estimation of $\|\tau\|$, and therefore in σ_h and τ_h. In version 2.3.1, the estimation of the maxima of σ_h is close to the observations. The absence of turbulence feedback on the mean flow induces an obvious sensitivity to vertical resolution. Significant vertical gradients at $z \approx H$ lead to a notable decrease in τ_h.

Figure 1: Wind and turbulence modeled (τ_h, τ_h) in a wind tunnel (dashed lines) and by PSWIFT (solid lines)

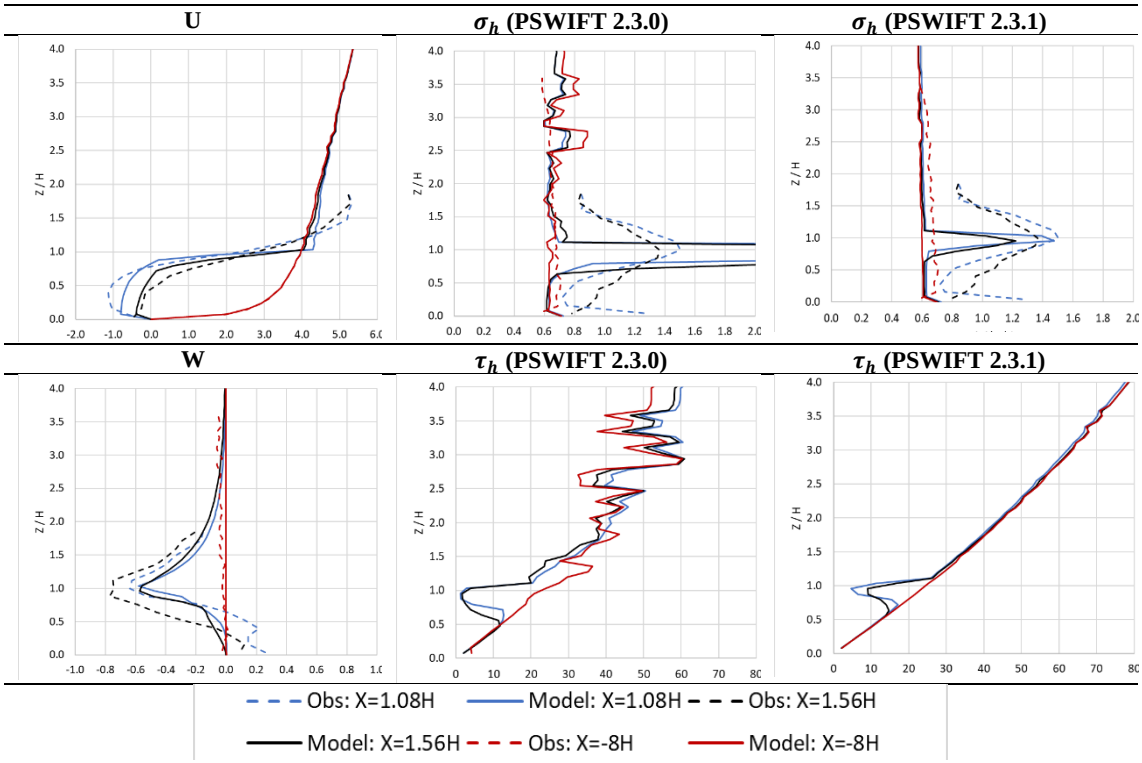

ACADEMIC CASE STUDY OF A FOREST IN THE MIDDLE OF A PRAIRIE

The canopy is defined as the SBL containing a set of obstacles around which air circulates. The vegetation canopy describes the presence of cultivated fields or wooded areas. Cionco (1965) models the progressive absorption of momentum within a vegetation canopy using an exponential law. A wide range of experimental data validates the formulation (Cionco, 1972), also the urban canopy (MacDonald, 2000).
Noting h_c as the height of the canopy, and D_c as an empirical coefficient of wind attenuation (known as canopy density), the exponential decrease within the canopy is modeled by the equation below. The profile within the canopy tends towards 0 for a high attenuation coefficient D_c.

$$u(z) = u(h_c) \cdot \exp\left(-D_c \cdot \left(1 - \frac{z}{h_c}\right)\right)$$

The implementation of canopy attenuation in PSWIFT follows that of SCICHEM (Version 3.2.2, 2019), which is justified because it reproduces the experimental data collected by Cionco (1972). The wind is analytically modified over a thickness $2 \cdot h_c$. The values h_c and D_c required for parameterization are specified in the file detailing land use in the modeled area.
An academic case study on flat terrain illustrates the influence of the canopy on the wind by simulating a small forest (0.5km x 0.5km) surrounded by grassland (2.5km x 2.5km). The atmosphere corresponds to case number 17 of the Prairie Grass experiment, with a northward wind (Ribstein et al., 2024). The forest is defined by ($h_c = 15m, D_c = 2$). A uniform vertical resolution of 1m is chosen up to 100m.
A parameterization of the canopy modifies the interpolated wind before applying the mass conservation constraint, thereby creating a slight deflection around the forest. The influence of the canopy extends only slightly horizontally and vertically. Figure 2 also demonstrates that the attenuation of the wind field does not change when the horizontal resolution decreases from dx=50m to dx=5m.
In version 2.3.0, the rate at which the wind recovers above the canopy ($h_c \leq z \leq 2 \cdot h_c$) is parameterized by the roughness, which also characterizes SBL and, consequently, the turbulent profiles. In version 2.3.1, the rate depends solely on h_c and D_c (Kung, 1961). This correction decouples large-scale turbulence from the characteristics of smaller scales.
Figure 2 shows a series of extractions along a line crossing the forest, visualizing the vertical profiles of τ_h, with a color code transitioning from blue (grassland) to green (forest). In version 2.3.0, by imposing a roughness variation from 0.006m (grassland) to 1m (forest), the wind attenuation is consistent but is accompanied by a 2.6-fold increase in u_*, leading to a notable increase in (σ_h ; σ_z) and a decrease in

(τ_h ; τ_z). By neglecting the forest's impact on large-scale turbulence (uniform roughness), version 2.3.1 maintains the consistency of wind attenuation in the canopy and avoids turbulence jumps. Finally, it is noted that the formulation based on a mixing length modifies the turbulent quantities only where wind attenuation introduces significant gradients, i.e., within the forest and for $z \leq 2 \cdot h_c$.

Figure 2: (Left) inlet wind profile (dashed line) and extracted profiles from the grassland (blue) and the forest (red); (Center and Right) extraction every 100 m of τ h profiles along a line passing through the center of the forest

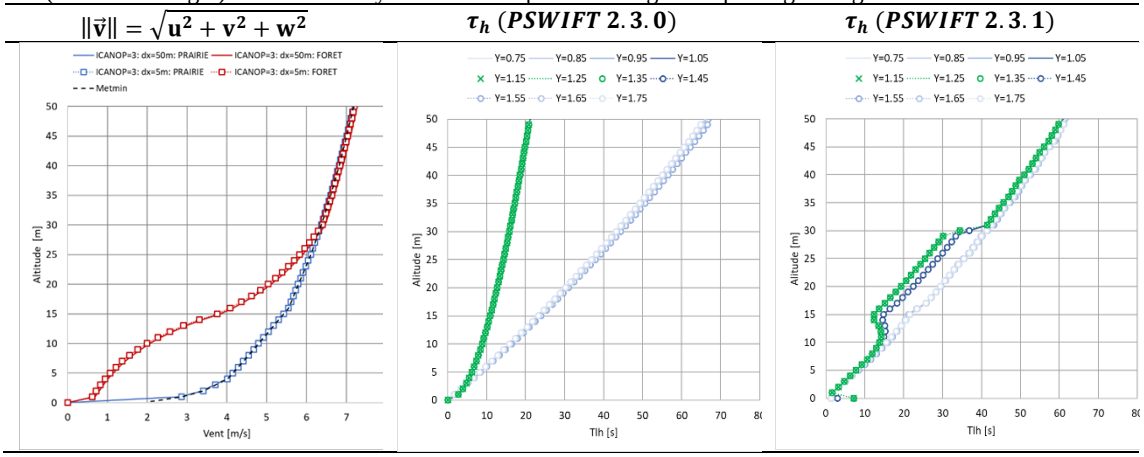

GENERAL CONCLUSION AND PERSPECTIVES

This paper has led to an intensive review of the PSWIFT source code, resulting in updates to the definition of Pasquill stability classes, a correction to the contribution of vertical gradients in the deformation tensor, and the ability to parameterize large-scale turbulence independently of smaller-scale characteristics, such as the vegetation canopy. The modifications and validations presented relate to the PSWIFT model. Armand et al. (2025) evaluates the impact of these changes on the PSPRAY dispersion model and demonstrate a significantly improved representation of background turbulence and turbulence induced by obstacles.

REFERENCES

Armand, P., O. Oldrini, C. Duchenne & S. Perdriel (2021) Topical 3D modelling and simulation of air dispersion hazards as a new paradigm to support emergency preparedness and response. *Environmental Modelling and Software*, 143, 105129.

Armand, P., Ribstein, B., Duchenne, C., Nibart, M., Albergel, A. (2025) Wind tunnel and in-field experimental validation of the recent developments on multi-scale turbulence in the PMSS modelling system. *Proc. of the 23rd Int. Conf. on Harmonisation within Atmospheric Dispersion Modelling for Regulatory Purposes*. 15-19 September 2025, Hamburg, Germany.

Cionco, R.M. (1962). A preliminary model for air flow in the vegetative canopy. *Bull. Amer. Meteor. Soc*., 43, 319.

Cionco, R.M. (1972). A wind-profile index for canopy flow. *Boundary Layer Meteorology*, 3, 255-263

CEDVAL. *https://www.mi.uni-hamburg.de/en/arbeitsgruppen/windkanallabor/data-sets.html*

Fackrell, J.E. (1984). Parameters characterizing dispersion in the near wake of buildings. *Journal of Wind Engineering and Industrial Aerodynamics*, 16, 97-118.

Golder D. (1972). Relations among stability parameters in the surface layer. *Boundary-Layer Meteorol*., 3: 56.

Hanna S. R., Briggs G. A., Hosker R. P. (1982) Handbook on atmospheric diffusion. Ed. by J. S. Smith, U.S. Department of Energy.

Horst T. W., Doran J. C., Nickola P. W. (1979). Evaluation of empirical atmospheric diffusion data. Battelle Pacific Northwest Lab.

Kung, E.C. (1961). Derivation of Roughness Parameters from Wind-drolly Data Over Tall Vegetation. In: *Report on Studies of the Three-Dimensional Nature of the Planetary Boundary Layer*, Department of Meteorology, University of Wisconsin.

MacDonald, R.W. (2000). Modelling the mean velocity profile in the urban canopy layer. *Boundary Layer Meteorology*, 97, 25-45

Monin, A.S, Obukhov, A.M. (1954). Basic laws of turbulent mixing in the surface layer of the atmosphere. Tr. *Akad. Nauk. SSSR Geophiz. Inst.*, vol. 24, no 151, p. 163–187.

Oldrini, O., P. Armand, C. Duchenne & S. Perdriel (2019) Parallelization performances of PMSS flow and dispersion modeling system over a huge urban area. *Atmosphere*, 10 (7), 404.

Oldrini, O., P. Armand, C. Duchenne, S. Perdriel & M. Nibart (2021) Accelerated time and high-resolution 3D modeling of the flow and dispersion of noxious substances over a gigantic urban area – EMERGENCIES project. *Atmosphere*, 12 (5), 640-654.

Ribstein, B., Armand, P., Duchenne, C., Yang, X., David, V., Nibart, M., Albergel, A. (2024) Proposals for improving the multi-scale consideration of turbulence in the PMSS diagnostic modelling system. *Proc. of the 22nd Int. Conf. on Harmonisation within Atmospheric Dispersion Modelling for Regulatory Purposes*. 10-14 June 2024, Pärnu, Estonia.

Rodean, H.C. (1996). Stochastic Lagrangian Models of Turbulent Diffusion. In: *American Meteorological Society Boston*, MA, 1, 1-84. Doi: 10.1007/978-1-935704-11-9.

SCICHEM, Version 3.2.2 (2019). Technical Documentation. EPRI, Palo Alto, CA. 3002016526

Smagorinsky, J. (1963) General circulation experiments with the primitive equations: I. The basic equations. *Mon. Weather Rev*, 91, 99-164.

Tinarelli, G., L. Mortarini, S. Trini Castelli, G. Carlino, J. Moussafir, C. Olry, P. Armand & D. Anfossi (2013) Review and validation of Micro-SPRAY, a Lagrangian particle model of turbulent dispersion. In: *Lagrangian Modeling of the Atmosphere*, Geophysical Monograph, American Geophysical Union, 200, 311-327, May 2013, Washington DC.